Two-Level MPPM–*M*DPSK Modulation for Free-Space Optical Channels

Abdulaziz E. Elfiqi[1], Ahmed E. Morra[1,2], Haitham S. Khallaf[3], Hossam M. H. Shalaby[4,5], Steve Hranilovic[2]

[1] Faculty of Electronic Engineering (FEE), Menoufia University, Menouf 32952, Egypt

[2]Department of Electrical and Computer Engineering, McMaster University, Ontario L8S 4K1, Canada

[3]Nuclear Research Center, Egyptian Atomic Energy Authority (EAEA), Inshas 13759, Egypt

[4]Egypt-Japan University of Science and Technology (E-JUST), Alexandria 21934, Egypt

[5]Electrical Engineering Department, Alexandria University, Alexandria 21544, Egypt

abdulaziz.elfiqi@ieee.org, morraa1@mcmaster.ca, eng.h.khallaf@gmail.com, shalaby@ieee.org, hranilovic@mcmaster.ca

***Abstract*—A hybrid two-level multipulse pulse-position modulation–*M*-ary differential phase-shift keying (2*L*-MPPM–*M*DPSK) technique is proposed which achieves high power and spectral efficiencies. The proposed 2*L*-MPPM–*M*DPSK scheme is shown to have the highest spectral efficiency in comparison with other hybrid modulation schemes. Additionally, the proposed technique has the advantage of removing the complex variable delay-line required for the direct-detection of other hybrid MPPM-*M*DPSK systems. The performance of 2*L*-MPPM–*M*DPSK is quantified in free-space optical (FSO) channels modeled with an exponentiated Weibull (EW) fading distribution. Closed-from expressions for both bit-error rate (BER) and outage probability upper-bound are derived and verified using Monte Carlo (MC) simulation. At the same data rate and bandwidth, 2*L*-MPPM–*M*DPSK techniques outperform traditional MPPM–*M*DPSK scheme by approximately 2 dB at a BER of 10^{-4}.**

I. Introduction

Hybrid modulation techniques have advantages over traditional modulation techniques as they can transmit data with both high spectral and power efficiencies simultaneously. This is gained by combining the advantages of both power efficient position based-modulation techniques and spectrally efficient phase based-modulation techniques [1]–[13]. One of the most promising hybrid modulation techniques combines multipulse pulse-position modulation (MPPM) with M–ary differential phase-shift keying (MDPSK) to give hybrid MPPM–MDPSK [6], [7]. This technique, however, requires an ultrafast optical variable delay line in order to be directly detected which greatly increases its complexity.

This work introduces a lower complexity hybrid modulation scheme in which the MPPM signal has two non-zero amplitudes allowing the DPSK to be sent continuously thus overcoming the need for variable delays. This *two-level* ($2L$) $2L$-MPPM–MDPSK approach simultaneously provides high spectral efficiency with good power efficiency and a greatly simplified transmitter and receiver in comparison with other hybrid modulation schemes [1]–[12]. A literature survey of existing hybrid modulation works with notation to the receiver complexity is summarized in Table I.

Although free-space optical (FSO) communication systems offer many advantages such as large data rates and unregulated spectrum, they are greatly impaired by atmospheric conditions [14], [15]. Both turbulence-induced scintillation fading and attenuation from fog are two important impairments affecting FSO performance.

TABLE I
Survey of Hybrid modulation techniques considering receiver complexity.

Technique	Detection type	All-optical receiver?
[1]–[4], [12]	Coherent (PSK+PPM/MPPM)	Yes
[10], [11]	Direct (QAM+MPPM)	No
[6], [7]	Direct (DPSK+MPPM, var. delay-line)	Yes
This work	Direct (DPSK+MPPM)	Yes

In this paper, we apply $2L$-MPPM–MDPSK hybrid modulation techniques to FSO links in order to increase their deployment ranges and improve their reliability. The spectral and power efficiencies of $2L$-MPPM–MDPSK are studied and compared with that of earlier hybrid MPPM-*M*DPSK schemes. The effects of the FSO channel on the bit-error rate (BER) and the outage performance of $2L$-MPPM–MDPSK are investigated under exponentiated Weibull (EW) distribution [16].

The balance of the paper is organized as follows. In Section II, $2L$-MPPM–MDPSK is defined and the structures of both transmitter and receiver are outlined. Furthermore, the spectral and power efficiencies are investigated. In Section III, the BER and the outage probability for the $2L$-MPPM–MDPSK system under EW-turbulence FSO fading channels are derived. Simulation results and comparisons are presented in Section IV. Finally, the conclusions are drawn in Section V.

II. Definition of Hybrid $2L$-MPPM–MDPSK Scheme

1) Definition: Schematic block diagrams of both transmitter and receiver of proposed $2L$-MPPM–MDPSK scheme are shown in Fig. 1.

At the transmitter, a data frame with a length of $\left\lfloor \log_2 \binom{N}{w} \right\rfloor + N \log_2 M$ bits is fed to the transmitter signal-processing unit (T-SPU), where w is the number of time-slots

978-1-5386-4727-1/18/$31.00 ©2018 IEEE

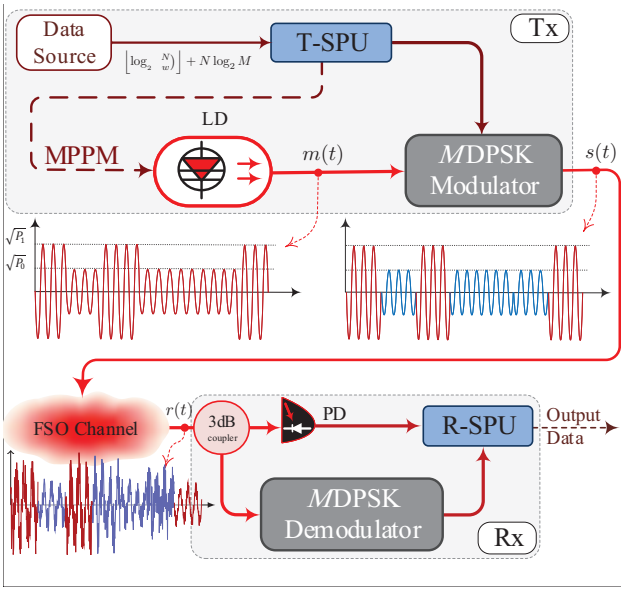

Fig. 1. Block-diagram of proposed hybrid $2L$-MPPM–MDPSK. Tx: Transmitter, Rx: Receiver, LD: Laser diode, PD: Photodiode, T-SPU: Transmitter signal-processing unit, R-SPU: Receiver signal-processing unit. The illustrated transmitted waveform has parameters $(N, w, M, \delta) = (8, 3, 2, 0.25)$.

with high signal-level in N time-slots of the MPPM frame and M is the number of modulation levels of MDPSK. The T-SPU manipulates these bits to control the operation of both the laser diode (LD) driving current (i.e., MPPM signal) and MDPSK modulator.

The MPPM signal is carried by intensity modulating the optical carrier with two power levels P_0 and P_1 where $P_0 < P_1$. That is, the $\left\lfloor \log_2 \binom{N}{w} \right\rfloor$ information bits are carried in the positions of w pulses, transmitted at power level P_1, while the remaining $N - w$ pulses are transmitted at a power level P_0. Define δ as the inverse of the *transmitter extinction ratio*, i.e.,

$$\delta = \frac{P_0}{P_1}. \tag{1}$$

Thus the k-th time slot of $2L$MPPM modulated optical signal can be represented as

$$m_k(t) = a_k \exp\left(j\omega_c t\right), \tag{2}$$

where ω_c is the optical carrier frequency in rad/s and $a_k \in \{\sqrt{P_0}, \sqrt{P_1}\}$ as shown in Fig. 1. The remaining $N \log_2 M$ information bits are carried by the differential phase modulation of $m_k(t)$ using an optical MDPSK modulator. The k-th time slot of the $2L$-MPPM–MDPSK transmitted optical signal is expressed as

$$s_k(t) = a_k \exp\left(j(\omega_c t + \phi_k)\right), \tag{3}$$

where ϕ_k is the phase conveyed by MDPSK modulator which corresponds to phase difference

$$\Delta\phi_k = \phi_k - \phi_{k-1} = (2i-1)\pi/M$$

where $i \in \{1, 2, \ldots, M\}$, as illustrated in Fig. 1.

TABLE II
SPECTRAL EFFICIENCIES FOR DIFFERENT MPPM- AND MDPSK-BASED MODULATION TECHNIQUES IN [bit/s/Hz]

Modulation Scheme	Spectral Efficiency, η_s [bit/s/Hz]
MDPSK	$\log_2 M$
MPPM	$\frac{\left\lfloor \log_2 \binom{N}{w} \right\rfloor}{N}$
MPPM–MDPSK [6], [7]	$\frac{\left(\left\lfloor \log_2 \binom{N}{w} \right\rfloor + w \log_2 M\right)}{N}$
$2L$-MPPM–MDPSK	$\frac{\left(\left\lfloor \log_2 \binom{N}{w} \right\rfloor + N \log_2 M\right)}{N}$

At the receiver, considering the FSO channel gain, h, the received signal

$$r_k(t) = \sqrt{h} a_k \exp\left(j(\omega_c t + \phi_k)\right), \tag{4}$$

is spilt by a 3 dB coupler into two branches: one for MPPM and the other for MDPSK demodulation. Given that the coherence time of atmospheric fading is many orders of magnitude larger than the symbol interval, we adopt a non-ergodic model for the channel fading state and represent it as independent of time and EW distributed [14].

In the MPPM arm, the photodiode (PD) converts the optical intensity variation into an electrical signal that is fed to the receiver signal-processing unit (R-SPU). The R-SPU detects the received data by collecting N consecutive slot intervals and independently detecting the positions of the w high signal-level time-slots that contain the highest power.

In the MDPSK arm, traditional direct detection for the MDPSK signal is performed by employing optical delay interferometers. It should be noted that independent data is sent over the MDPSK branch in each of the N slots of the MPPM symbol. This is the key point in simplifying the receiver for $2L$-MPPM–MDPSK since variable delay lines are not required for DPSK detection as in [6], [7]. In the R-SPU, the received data words are reconstructed independently from both the $2L$MPPM and MDPSK decoded bits.

It worth mentioning that the position based- and phase based-modulation techniques are transmitted independently in contrast to the previous hybrid modulation techniques [1]–[4], [6], [7], [10]–[12], which results in simplified T-SPU and R-SPU for the proposed $2L$-MPPM–MDPSK modulation technique since no time synchronization is needed between MPPM and MDPSK branches.

2) Spectral and Power Efficiencies: As is conventional, define the spectral efficiency η_s as [17]

$$\eta_s = \frac{R_b}{B_\omega} \quad \text{bit/s/Hz}, \tag{5}$$

where R_b is the transmission data rate in bits per second, $B_\omega = 1/\tau$ is the receiver bandwidth, $\tau = T/N$ is the time slot duration and T is the frame time duration. The spectral efficiencies of different MPPM- and MDPSK-based modulation techniques are summarized in Table II. It can be observed that, for a given N, w and M, $2L$MPPM-MDPSK technique has the highest spectral efficiency in comparison

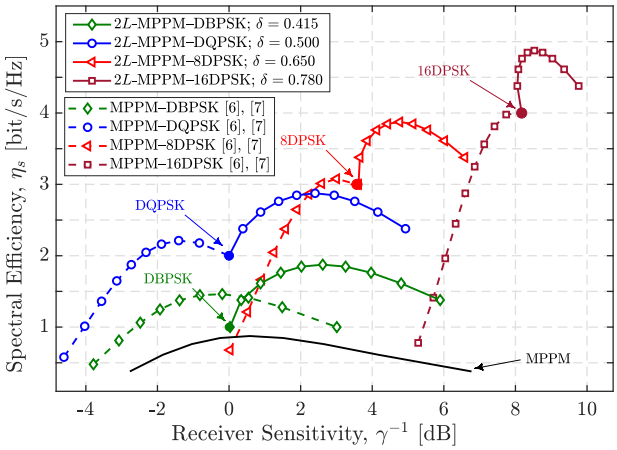

Fig. 2. Achieved spectral efficiencies of different MPPM- and MDPSK-based modulation techniques versus the receiver sensitivity at different values of N/w ratio and different MDPSK cardinality level.

with other hybrid modulation techniques. Of course, this increased spectral efficiency comes at the expense of decreasing some of the power efficiency of MPPM for $\delta > 0$.

The power efficiency for modulation schemes is defined as [17]

$$\gamma = \frac{d_{\min}^2}{4\mathcal{E}_b}, \tag{6}$$

where $d_{\min}$ is the minimum Euclidean distance between two symbols in the constellation space and $\mathcal{E}_b$ is the average energy per bit. Following a similar approach as in [8], [9], the power efficiency for $2L$-MPPM–MDPSK scheme is

$$\gamma = \frac{\left\lfloor \log_2 \binom{N}{w} \right\rfloor + N \log_2 M}{w + (N-w)\delta^2} \min\left\{ \frac{(1-\delta)^2}{2}, \delta^2 \sin^2\left(\frac{\pi}{M}\right) \right\} \tag{7}$$

Figure 2 plots the spectral efficiencies in [bit/s/Hz] of different hybrid MPPM- and MDPSK-based modulation techniques versus the reciprocal of the power efficiency (i.e., the receiver sensitivity) in [dB] at different cardinality level of MDPSK modulation technique, i.e: $M \in \{2, 4, 8, 16\}$ with different values for $w/N \in [0:1]$. Notice that Figure 2 can be used as a design guide to select the hybrid modulation approach and parameters to maximize spectral efficiency for each receiver sensitivity.

It can be seen that the $2L$-MPPM–MDPSK technique has the highest power efficiency in the high spectral efficiency region ($\eta_s > 2.25$ bit/s/Hz). It worth mentioning that the maximum spectral efficiency for our $2L$ techniques at any cardinality of the MDPSK is achieved at a $w/N = 0.5$. Additionally the value of δ balances the power efficiency between MPPM and MDPSK. Notice that δ must increase with increasing M to balance the impact on power efficiency of increasing the cardinality of the DPSK modulation. The particular values of δ selected in Fig. 2 for the $2L$ techniques are found by optimizing to provide the best power efficiency when $w/N = 0.5$.

As compared to ordinary phase modulation approaches, these hybrid approaches increase complexity to both the transmitter and the receiver by superimposing MPPM with phase modulation techniques. However, the proposed hybrid techniques are useful not only to improve spectral efficiency, but are also practically well suited to time varying channels, e.g., free-space optical channels. In time-varying FSO channels, large irradiance fluctuations are possible between coherence times even in clear weather. Low rate data transmitted on the power efficient MPPM stream will be more robust to channel variations while data on the MDPSK branch will provide higher rates when conditions are favourable. Thus, this hybrid approach has the practical benefit of maintaining connectivity over channel variations.

III. Performance Analysis in FSO Fading Channels

In this section, the average BER and the outage probability of proposed $2L$-MPPM–MDPSK over exponentiated Weibull (EW) distributed turbulence FSO channels are investigated and discussed.

A. EW-Turbulence FSO Channel Model

Several statistical distributions have been developed to characterize the impact of atmospheric turbulence on communications channels in the literature. Some widely accepted distributions are log-normal (LN), gamma-gamma (GG), and exponentiated Weibull (EW) models [16]. Under a wide range of aperture averaging and turbulence conditions, the EW model provides an excellent match with the simulation and experimental data. Moreover, the EW distribution has the attractive feature of having a relatively simple probability density function (PDF) and a cumulative distribution function (CDF) in closed form expressions.

The FSO channel gain, h, PDF and CDF under EW channel model can be written as [16]

$$f_h(h) = \frac{\alpha\beta}{\eta}\left(\frac{h}{\eta}\right)^{\beta-1} \exp\left(-\left(\frac{h}{\eta}\right)^{\beta}\right) \times \left[1 - \exp\left(-\left(\frac{h}{\eta}\right)^{\beta}\right)\right]^{\alpha-1}, \tag{8}$$

$$F_h(h) = \left[1 - \exp\left(-\left(\frac{h}{\eta}\right)^{\beta}\right)\right]^{\alpha}, \tag{9}$$

respectively, where the receiver aperture size-based extra shape parameter α, the scintillation index-based shape parameter β, and the scale parameter η, are expressed as

$$\alpha \approx 3.931\,(D_R/\rho_o)^{-0.519}, \tag{10}$$

$$\beta \approx \left(\alpha\sigma_I^2\right)^{-6/11}, \tag{11}$$

$$\eta = \frac{1}{\alpha\Gamma(1+\frac{1}{\beta})g(\alpha,\beta)}, \tag{12}$$

respectively, where σ_I^2 is the scintillation index, $\rho_o = (1.46C_n^2(2\pi/\lambda)^2 L_t)^{-3/5}$ is the atmospheric coherence radius, λ is the transmission wavelength, L_t is the FSO link length, C_n^2

is the refractive-index structure constant, D_R is the aperture diameter, $\Gamma(\cdot)$ is the gamma function and $g(\alpha,\beta)$ is defined as

$$g(\alpha,\beta)=\sum_{i=0}^{\infty}\frac{(-1)^i(i+1)^{-(1+\beta)/\beta}\Gamma(\alpha)}{i!\Gamma(\alpha-i)}. \tag{13}$$

Using Newton's generalized-binomial theorem and expressing $\exp(\cdot)$ in terms of MeijerG function, $\mathrm{G}_{p,q}^{a,b}\left(\cdot\middle|\begin{smallmatrix}\cdot\\ \cdot\end{smallmatrix}\right)$, via [18, Eq. (07.34.03.0228.01)], (8) can be written as

$$f_h(h)=\frac{\alpha\beta}{\eta}\left(\frac{h}{\eta}\right)^{\beta-1}\sum_{j=0}^{\infty}\frac{(-1)^j\Gamma(\alpha)}{j!\Gamma(\alpha-j)}\mathrm{G}_{0,1}^{1,0}\left((1+j)\left(\frac{h}{\eta}\right)^{\beta}\middle|\begin{smallmatrix}-\\ 0\end{smallmatrix}\right) \tag{14}$$

B. Upper-Bound BER Analysis

The $2L$MPPM symbol consists of w high signal-level time-slots with a power level of P_1 and $N-w$ low signal-level time-slots with a power level of $P_0=\delta P_1$, where $0<\delta<1$. The average transmitted optical power P_{av} is defined as

$$P_{av}=\frac{w+\delta(N-w)}{N}P_1. \tag{15}$$

The upper-bound BER expressions can be derived based on union-bound that is expressed as follows [19]

$$\mathrm{BER}\le\frac{\nu}{4}\operatorname{erfc}\left(\frac{d_{\min}}{2\sqrt{N_0}}\right), \tag{16}$$

where $N_0/2$ is the power spectral density of the noise and ν is the cardinality of the constellation with $\nu=\binom{N}{w}$ and M for $2L$MPPM and MDPSK techniques, respectively. The minimum Euclidean-distance between any two points in the signal constellation is $d_{\min}$, which is expressed as follows

$$d_{\min}(h)=\mathcal{R}P_1h\times\begin{cases}\frac{(1-\delta)\sqrt{\tau}}{\sqrt{2}}; & \text{for } 2L\text{MPPM},\\ \delta\sin(\pi/M)\sqrt{\tau}; & \text{for } M\text{DPSK}.\end{cases} \tag{17}$$

where $\mathcal{R}$ is the detector responsivity. Accordingly, the upper-bound BER can be written as follows

$$\mathrm{BER}(h)\le\frac{\nu}{4}\operatorname{erfc}\left(\frac{CP_{av}}{\sigma_n}h\right), \tag{18}$$

where σ_n^2 is the noise variance, C is given as follows

$$C=\begin{cases}\frac{\mathcal{R}(1-\delta)N}{4(w+(N-w)\delta)}, & \text{for } 2L\text{MPPM};\\ \frac{\mathcal{R}\delta\sin(\pi/M)N}{\sqrt{8}(w+(N-w)\delta)}, & \text{for } M\text{DPSK}.\end{cases} \tag{19}$$

By expressing $\operatorname{erfc}(\cdot)$ in (18) in terms of MeijerG function, $\mathrm{G}_{p,q}^{a,b}\left(\cdot\middle|\begin{smallmatrix}\cdot\\ \cdot\end{smallmatrix}\right)$, using [18, Eq. (07.34.03.0619.01)], the BER can be written as

$$\mathrm{BER}(h)\le\frac{\nu}{4\sqrt{\pi}}\mathrm{G}_{1,2}^{2,0}\left(\left(\frac{CP_{av}}{\sigma_n}h\right)^2\middle|\begin{smallmatrix}1\\ 0,0.5\end{smallmatrix}\right). \tag{20}$$

Notice that the average BER over FSO fading states, BER^{av} can be obtained from

$$\mathrm{BER}^{av}=\int_0^{\infty}\mathrm{BER}(h)f_h(h)\,\mathrm{d}h. \tag{21}$$

By substituting (20) and (14) into (21) and using [20, Eq. (21)], the average BER can be written as (22) at the bottom of the page, where l and k are integers with $\frac{l}{k}=\frac{\beta}{2}$ and $\Delta(b,a)=\frac{a}{b},\frac{a+1}{b},\cdots,\frac{a+b-1}{b}$.

Finally, the average BER for the overall hybrid system is given by

$$\mathrm{BER}_{2L\text{MPPM-}M\text{DPSK}}^{av}=\frac{\lfloor\log_2\binom{N}{w}\rfloor\,\mathrm{BER}_{2L\text{MPPM}}^{av}+N\log_2 M\,\mathrm{BER}_{M\text{DPSK}}^{av}}{\lfloor\log_2\binom{N}{w}\rfloor+N\log_2 M}, \tag{23}$$

where $\mathrm{BER}_{2L\text{MPPM}}^{av}$ and $\mathrm{BER}_{M\text{DPSK}}^{av}$ can be obtained from (22) for different values of C given from (19).

C. Outage Probability Analysis

The outage probability is defined as

$$\mathrm{P}_{\mathrm{out}}=\Pr(\mathrm{BER}\ge\mathrm{BER}_{\mathrm{th}})=\Pr(h\le h_{\mathrm{th}}), \tag{24}$$

where h_{th} is the threshold channel gain that guarantees a minimum level of link quality (i.e., $\mathrm{BER}_{\mathrm{th}}$). Rearranging (18), h_{th} can be bounded as

$$h_{\mathrm{th}}\le\frac{\sigma_n}{CP_{av}}\operatorname{erfc}^{-1}\left(\frac{4\,\mathrm{BER}_{\mathrm{th}}}{\nu}\right). \tag{25}$$

Thus, the outage probability can be bounded using (9) as

$$\begin{aligned}P_{\mathrm{out}}&=\int_0^{h_{\mathrm{th}}}f_h(h)\,\mathrm{d}h=F_h(h_{\mathrm{th}})\\ &\le\left[1-\exp\left(-\left(\frac{\sigma_n}{C\eta P_{av}}\operatorname{erfc}^{-1}\left(\frac{4\,\mathrm{BER}_{\mathrm{th}}}{\nu}\right)\right)^{\beta}\right)\right]^{\alpha}.\end{aligned} \tag{26}$$

Finally, the outage probability upper-bound of the FSO systems adopting $2L$-MPPM–MDPSK schemes is

$$\mathrm{P}_{\mathrm{out}}^{2L\text{-MPPM}-M\text{DPSK}}\le 1-\left(1-\mathrm{P}_{\mathrm{out}}^{2L\text{MPPM}}\right)\left(1-\mathrm{P}_{\mathrm{out}}^{M\text{DPSK}}\right). \tag{27}$$

IV. Results and Discussions

In this section, the BER and outage probability of FSO systems adopting $2L$-MPPM–MDPSK techniques are numerically evaluated using (23) and (27), respectively. All results are verified through a Monte Carlo (MC) simulation by directly generating fading states and averaging. An operating wavelength of $\lambda=785\,\mathrm{nm}$ is selected so that silicon PDs can be used in order to decrease the receiver cost. Moderate

$$\mathrm{BER}^{av}\le\frac{\nu\alpha\beta\Gamma(\alpha)}{\sqrt{32l}}\left(\frac{P_{av}}{\sigma_n}\eta C\right)^{-\beta}\sqrt{\frac{kl^{\beta}}{(2\pi)^{l+k-1}}}\sum_{j=0}^{\infty}\frac{(-1)^j}{j!\Gamma(\alpha-j)}\mathrm{G}_{2l,k+l}^{k,2l}\left(\left(\tfrac{1+j}{k}\right)^k\left(\frac{\sqrt{l}\sigma_n}{CP_{av}\eta}\right)^{2l}\middle|\begin{smallmatrix}\Delta(l,1-\frac{\beta}{2}),\ \Delta(l,0.5-\frac{\beta}{2})\\ \Delta(k,0),\ \Delta(l,-\frac{\beta}{2})\end{smallmatrix}\right) \tag{22}$$

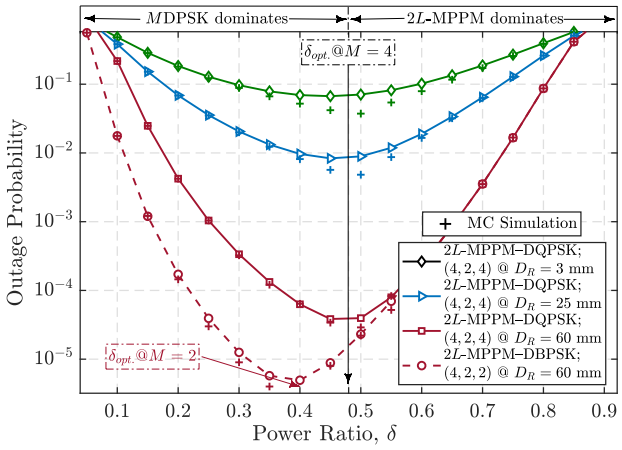

Fig. 3. Outage probabilities versus the power ratio δ for $2L$-MPPM–MDPSK with parameters (N, w, M) at $P_{av} = -15\,\text{dBm}$ and $\sigma_n^2 = 25 \times 10^{-14}\ A^2$ for different aperture sizes and $\text{BER}_{\text{th}} = 10^{-3}$. MC simulations (+) are also plotted.

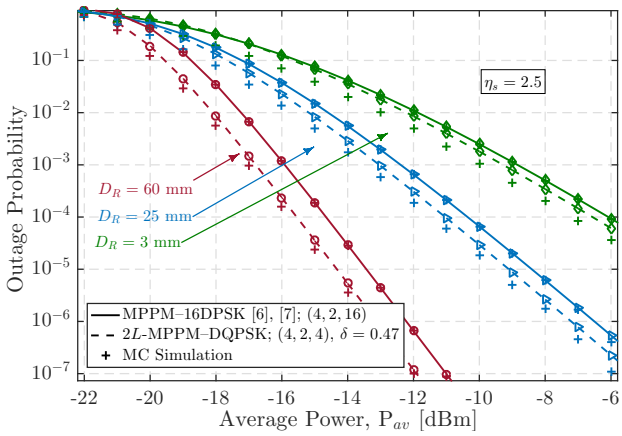

Fig. 4. Outage probability versus P_{av} (dBm) for both $2L$-MPPM–MDPSK with $(N, w, M, \delta, \eta_s) = (4, 2, 4, 0.47, 2.5)$ and MPPM–MDPSK with $(N, w, M, \eta_s) = (4, 2, 16, 2.5)$ for different aperture sizes at $\sigma_n^2 = 25 \times 10^{-14}\ A^2$ and $\text{BER}_{\text{th}} = 10^{-3}$. MC simulations (+) are also plotted.

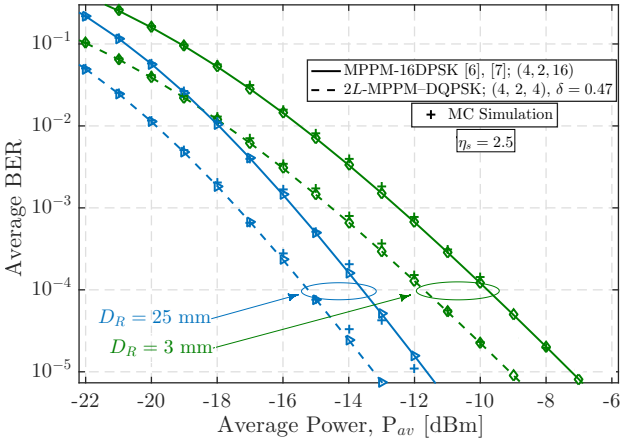

Fig. 5. Average BER versus P_{av} (dBm) for both $2L$-MPPM–MDPSK with $(N, w, M, \delta, \eta_s) = (4, 2, 4, 0.47, 2.5)$ and MPPM–MDPSK with $(N, w, M, \eta_s) = (4, 2, 16, 2.5)$ for different aperture sizes at $\sigma_n^2 = 25 \times 10^{-14}\ A^2$. MC simulations (+) are also plotted.

turbulence is considered with $C_n^2 = 2.128 \times 10^{-14}\ \text{m}^{-2/3}$, $L = 1.2\,\text{km}$, Rytov variance $\sigma_R^2 = 1.3089$ and $\rho_o = 9.4\,\text{mm}$. The effect of aperture-averaging takes place if $D_R >> \rho_o$. In order to investigate the effect of aperture-averaging on FSO system performance, three different aperture sizes are considered in this section ($D_R = 3\,\text{mm}$, $\alpha = 5.44$, $\beta = 0.76$, $\eta = 0.31$), ($D_R = 25\,\text{mm}$, $\alpha = 4.65$, $\beta = 1.17$, $\eta = 0.52$) and ($D_R = 60\,\text{mm}$, $\alpha = 3.19$, $\beta = 2.61$, $\eta = 0.82$) [21].

Figure 3 shows the effect of changing the power ratio δ on outage probabilities. From (25) and (19), we can see that the outage performance of $2L$MPPM technique is improved by decreasing δ while MDPSK outage is improved by increasing δ. At low δ, MDPSK dominates outage, therefore, by increasing δ the complete system performance is improved until an optimum point is reached balancing the outage of MDPSK and MPPM. Increasing δ beyond this optimum, results in MPPM dominating outage and thus total system performance is again degraded.

Figures 4 and 5 show, respectively, the outage probability and the average BER versus the average transmitted optical power P_{av} for both proposed $2L$-MPPM–MDPSK and traditional MPPM–MDPSK techniques with δ fixed at the optimum value in Fig. 3. To permit a fair comparison, the parameters are chosen so that both systems have same transmission data rate, same average energy, and same bandwidth. Specifically, in Figs. 4 and 5, the two techniques use the same MPPM parameters $(N = 4, w = 2)$ but the MPPM–MDPSK technique [6], [7] uses a higher cardinality $M = 16$ than that of $2L$-MPPM–MDPSK technique to compensate for its lower spectral efficiency.

It can be seen that $2L$-MPPM–MDPSK outperforms MPPM–MDPSK by approximately $2\,\text{dB}$ at $\eta_s = 2.5\,\text{bit/s/Hz}$ and an average BER of 10^{-4} for all aperture sizes. This can be explained as follows. The proposed $2L$-MPPM–MDPSK scheme sends a DPSK symbol every τ slot interval while MPPM–MDPSK scheme sends only w DPSK symbols per frame. Therefore, in order to have the same spectral efficiency, MPPM–MDPSK must send higher cardinality DPSK constellations $M = 16$, that decreases the minimum Euclidean-distance. Finally, it can be seen from Figs 3, 4 and 5 that for $D_R < \rho_o$, the receiving aperture is unable to average turbulence while for the diameters, i.e; $D_R > \rho_o$, the aperture-averaging effect starts to appear and the system performance is improved by increasing the aperture diameter.

V. Conclusions

A simple direct-detection hybrid modulation technique ($2L$-MPPM–MDPSK) has been proposed. The proposed technique combines the benefits of both MPPM and MDPSK. The key insight over previous hybrid approaches is that an MDPSK symbol is sent each slot interval at the cost of losing some power efficiency of the MPPM sub-modulation. The performance of $2L$-MPPM–MDPSK over an FSO system has been investigated under EW distributed fading. Closed-form

expressions for both the outage probability and BER upper-bound have been derived. The obtained expressions are used for evaluating and comparing our proposed technique with the traditional hybrid MPPM–MDPSK and are also verified via MC simulations.

The results indicate that $2L$-MPPM–MDPSK techniques provide superior power efficiencies at high spectral efficiency region ($\eta_s > 2.25\,\mathrm{bit/s/Hz}$) while simultaneously reducing the complexity over earlier hybrid modulation approaches. Specifically, at $\eta_s = 2.5\,\mathrm{bit/s/Hz}$, the proposed $2L$-MPPM–MDPSK has a power saving of approximately $2\,\mathrm{dB}$ at a BER of 10^{-4}.

REFERENCES

[1] X. Liu, S. Chandrasekhar, T. H. Wood, R. W. Tkach, P. J. Winzer, E. C. Burrows, and A. R. Chraplyvy, "M-ary pulse-position modulation and frequency-shift keying with additional polarization/phase modulation for high-sensitivity optical transmission," *Opt. Express*, vol. 19, no. 26, pp. 868–881, Dec. 2011.

[2] X. Liu, T. H. Wood, R. W. Tkach, and S. Chandrasekhar, "Demonstration of record sensitivities in optically preamplified receivers by combining PDM-QPSK and M-ary pulse-position modulation," *J. Lightw. Technol.*, vol. 30, no. 4, pp. 406–413, Feb. 2012.

[3] T. A. Eriksson, P. Johannisson, B. J. Puttnam, E. Agrell, P. A. Andrekson, and M. Karlsson, "K-over-L multidimensional position modulation," *J. Opt. Commun. Netw.*, vol. 32, no. 12, pp. 2254–2262, June 2014.

[4] M. Sjodin, T. A. Eriksson, P. A. Andrekson, and M. Karlsson, "Long-haul transmission of PM-2PPM-QPSK at 42.8 Gbit/s," in *OFC/NFOEC Technical Digest*, Anaheim, CA, USA, March 2013, pp. 1–3.

[5] H. S. Khallaf, H. M. H. Shalaby, and Z. Kawasaki., "Proposal of a hybrid OFDM-PPM technique for free space optical communications systems," in *2013 IEEE Photonics Conference (IPC)*, Bellevue, WA, USA, Sept. 2013, pp. 287–288.

[6] A. E. Morra, H. M. H. Shalaby, S. F. Hegazy, and S. S. A. Obayya, "Hybrid direct-detection differential phase shift keying-multipulse pulse position modulation techniques for optical communication systems," *Opt. Commun.*, vol. 357, pp. 86–94, Dec. 2015.

[7] A. E. El-fiqi, A. E. Morra, S. F. Hegazy, H. M. H. Shalaby, K. Kato, and S. S. A. Obayya, "Performance evaluation of hybrid DPSK-MPPM techniques in long-haul optical transmission," *Appl. Opt.*, vol. 55, no. 21, pp. 5614–5622, July 2016.

[8] H. M. H. Shalaby, "Maximum achievable constrained power efficiencies of MPPM-LQAM techniques," *IEEE Photon. J.*, vol. 27, no. 12, pp. 1265–1268, June 2015.

[9] A. E. Morra, M. Rihan, A. E. El-Fiqi, H. M. H. Shalaby, and S. S. A. Obayya, "Evaluation of power efficiency of hybrid modulation techniques," in *2016 IEEE Photonics Conference (IPC)*, USA, Oct. 2016, pp. 33–34.

[10] H. S. Khallaf, H. M. H. Shalaby, J. M. Garrido-Balsells, and S. Sampei, "Performance analysis of a hybrid QAM-MPPM technique over turbulence-free and Gamma-Gamma free-space optical channels," *J. Opt. Commun. Netw.*, vol. 7, no. 2, pp. 161–171, Feb. 2017.

[11] H. S. Khallaf, A. E. Elfiqi, H. M. H. Shalaby, S. Sampei, and S. S. A. Obayya, "On the performance evaluation of LQAM-MPPM techniques over exponentiated Weibull fading free-space optical channels," *Opt. Commun.*, vol. 416, pp. 41–49, June 2018.

[12] H. Selmy, H. M. H. Shalaby, and Z. Kawasaki., "Proposal and performance evaluation of a hybrid BPSK-modified MPPM technique for optical fiber communications systems," *J. Lightw. Technol.*, vol. 31, no. 22, pp. 3535–3545, Nov. 2013.

[13] Y. Sun, F. Yang, and J. Gao, "Comparison of hybrid optical modulation schemes for visible light communication," *IEEE Photon. J.*, vol. 9, no. 3, pp. 1–13, June 2017.

[14] M. A. Khalighi and M. Uysal, "Survey on free space optical communication: A communication theory perspective," *Commun. Surveys Tuts.*, vol. 16, no. 4, pp. 2231–2258, Fourthquarter, 2014.

[15] A. E. Morra, K. Ahmed, and S. Hranilovic, "Impact of fiber nonlinearity on 5G backhauling via mixed FSO/Fiber network," *IEEE Access*, vol. 5, pp. 19 942–19 950, Sept. 2017.

[16] R. Barrios and F. Dios, "Exponentiated Weibull distribution family under aperture averaging for Gaussian beam waves," *Opt. Express*, vol. 20, no. 12, pp. 13 055–13 064, June 2012.

[17] S. Benedetto and E. Biglieri, *Principles of Digital Transmission: With Wireless Applications*. New York, NY, USA: Kluwer, 1999.

[18] *Wolfram Function Site. (2017, Sep.). [Online]. Available: http://functions.wolfram.com/.*

[19] S. Haykin, *Communication Systems*, 4th ed. New York, NY, USA: Wiley, 2001.

[20] V. S. Adamchik and O. I. Marichev, "The algorithm for calculating integrals of hypergeometric type functions and its realization in reduce system," in *Proc. of Int. Symposium on Symbolic and Algebraic Computation*, Tokyo, Japan, Aug. 1990, pp. 212–224.

[21] R. Barrios, "Exponentiated Weibull fading channel model in free-space optical communications under atmospheric turbulence," Ph.D., Universitat Politecnica de Catalunya, April 2013.